Direct Observation of a Long-Range Field Effect from Gate Tuning of Nonlocal Conductivity

Lin Wang,[1,2] Ignacio Gutiérrez-Lezama,[1,2] Céline Barreteau,[1] Dong-Keun Ki,[1,2] Enrico Giannini,[1] and Alberto F. Morpurgo[1,2]

[1]*Department of Quantum Matter Physics, University of Geneva, 24 quai Ernest-Ansermet, CH-1211 Geneva, Switzerland*

[2]*Group of Applied Physics, University of Geneva, 24 quai Ernest-Ansermet, CH-1211 Geneva, Switzerland*

(Received 19 May 2016; published 19 October 2016)

We report the direct observation of a long-range field effect in WTe_2 devices, leading to large gate-induced changes of transport through crystals much thicker than the electrostatic screening length. The phenomenon—which manifests itself very differently from the conventional field effect—originates from the nonlocal nature of transport in the devices that are thinner than the carrier mean free path. We reproduce theoretically the gate dependence of the measured classical and quantum magnetotransport, and show that the phenomenon is caused by the gate tuning of the bulk carrier mobility by changing the scattering at the surface. Our results demonstrate experimentally the possibility to gate tune the electronic properties deep in the interior of conducting materials, avoiding limitations imposed by electrostatic screening.

DOI: 10.1103/PhysRevLett.117.176601

Conventional field-effect transistors exploit electrostatic gating to tune the electronic properties of materials by means of charge accumulation [1–5]. Gate-induced charge accumulation occurs close to the material surface, on a depth limited by the so-called screening length, which is typically very short, ~1–2 nm. Electrostatic screening, therefore, seems to preclude the possibility to use field-effect transistor devices to control the electronic properties in the interior of materials, i.e., their bulk response. Although this is indeed the case in conventional field-effect devices, here we report the observation of a much longer-range field effect, affecting electronic transport through a material over a depth orders of magnitude longer than the electrostatic screening length. The phenomenon, which occurs because the electrical conductivity is governed by nonlocal processes, manifests itself in large gate-induced changes in the transport properties of conductors as long as their thickness is smaller than or comparable to the carrier mean free path.

We observe such a long-range field effect in crystals of WTe_2, a material possessing remarkable electronic properties [6–25]. Transport experiments have shown that bulk WTe_2 is a nearly perfectly compensated semimetal exhibiting record-high magnetoresistance (MR) because of the high electron and hole mobility [6,9,22]. They have also shown that whenever the crystal thickness is reduced below the mean free path (few hundreds of nanometers or even longer), the carrier mobility is suppressed by scattering at the surface [22]. As established long ago, this implies that transport at the microscopic scale is governed by nonlocal processes; i.e., the relation between current density and electric field is nonlocal [26–32]. It is well known that in this nonlocal regime different physical phenomena exhibit an unusual behavior, as illustrated by the so-called anomalous skin effect [33–35], i.e., the possibility for electromagnetic waves to penetrate into a conductor over a distance much larger than that predicted by the conventional theory. Although in the past it had been realized that gate tuning of surface scattering could result in the gate dependence of transport properties in systems—such as metals—in which no field effect should be expected [36,37], no direct experimental demonstration of this phenomenon and of its long-range nature has been provided [38].

Our devices consist of WTe_2 crystals with a thickness ranging from 10 to 50 nm exfoliated onto a highly doped silicon substrate covered with a 285 nm SiO_2 insulating layer [22]. The doped silicon substrate can be used as a gate electrode, even though for most devices—and certainly in the 50 nm thick crystals—no significant gate-induced modulation of transport is *a priori* expected. Indeed, applying a large gate voltage $V_g = 80$ V accumulates a charge of 8×10^{12} carriers/cm^2 at the surface, corresponding approximately to only (3–4)% of the total amount of charge carriers present in a 50 nm thick crystal. The resulting modulation in conductivity is expected to be even much smaller, as in a semimetal the gate voltage increases the surface density of one type of charge carriers and decreases that of the other, so that the effect on the conductivity largely compensates.

At odds with these expectations, Fig. 1 shows a pronounced effect of an applied V_g already on a 48 nm thick WTe_2 crystal (hereafter referred to as sample *A*). Figure 1(a) shows that the modulation in the Hall resistivity ρ_{xy} is so large that the sign of ρ_{xy} is inverted for magnetic field B up to 2–3 T. Even more surprisingly, the evolution of the low-B slope of ρ_{xy} is not consistent with the sign of the charges accumulated by the gate. Specifically, at a positive $V_g > 0$ V, electrons are accumulated, which

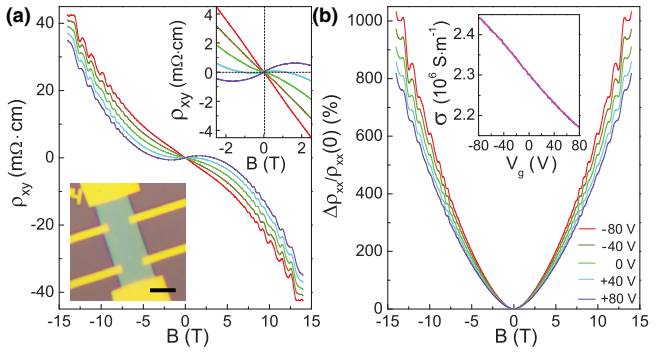

FIG. 1. Gate-induced modulation of magnetotransport in a 48 nm thick WTe_2 crystal (sample A). (a) Transverse resistivity ρ_{xy} showing a pronounced gate voltage V_g dependence [the curves of different color correspond to different values of V_g, as shown by the legend in panel (b)]. Note the change of sign occurring for $|B| < 3$ T, enlarged in the upper inset. The bottom inset shows an optical microscope image of the device (the bar is 5 μm). (b) V_g dependence of the longitudinal magnetoresistance (MR) of the same device. The inset shows the conductivity $\sigma(V_g)$ measured at $B = 0$ T. All data were taken at $T = 250$ mK.

should drive ρ_{xy} towards a negative slope. The inset of Fig. 1(a), however, shows the opposite behavior: the low-B slope of ρ_{xy} is negative at $V_g < 0$ V and becomes positive at $V_g = +80$ V. Furthermore, the conductivity σ measured at $B = 0$ T exhibits a V_g dependence opposite to that naively expected. Since we know from the analysis of magnetotransport at $V_g = 0$ V that in this device $\mu_e > \mu_h$ (see Ref. [22]), a positive V_g—which increases the electron density n and decreases the density of holes p—should slightly increase the total conductivity $\sigma = ne\mu_e + pe\mu_h$ (where μ_e and μ_h are electron and hole mobility). However, the inset of Fig. 1(b) shows that σ decreases upon driving V_g more positive. Therefore, electrostatic gating of a rather thick WTe_2 crystal results in sizable changes of the transport properties that are entirely inconsistent with the effect expected due to the accumulated surface charges, i.e., with the behavior of conventional field effect.

A hint to explain the observed gate-dependent behavior comes from the longitudinal MR measurements. Figure 1(b) shows that the MR, while being modulated by V_g, keeps exhibiting a quadratic dependence on B, consistent with $(\Delta\rho_{xx}/\rho_{xx}) = (\rho_{xx}(B) - \rho_{xx}(0)/\rho_{xx}(0)) = \mu_e\mu_h B^2$ [22]. This relation indicates that the MR depends only on μ_e and μ_h, suggesting that the observed V_g dependence of transport originates from a modulation of the mobility of the bulk carriers. This is possible because for all devices investigated here the electron and hole mean free paths ($L_e \sim L_h = \mu_{e,h}\hbar k_F/e$) are larger than the WTe_2 crystal thickness [39], so that the carrier mobility in the bulk is nonlocally determined by the scattering at the surface [22].

To understand physically how gating can affect the mobility of bulk carriers, it is sufficient to look at the gate-induced bending of the valence and conduction band near the material surface (see Fig. 2). At $V_g = 0$ V [Fig. 2(b)], the Fermi energy E_F is located inside the overlapping conduction and valence band uniformly throughout the entire thickness of the crystal, all the way up to the surface next to the gate dielectric. Electrons and holes move freely in the bulk and can reach the surface, where—as we know from past work [22]—they undergo scattering processes that determine their mobility μ_e and μ_h. Although the precise mechanism is yet unknown, all observations [22] indicate that the surface scattering is short ranged and mainly affects electrons reaching the outermost layer. A negative $V_g < 0$ V [Fig. 2(c)] increases the electrostatic energy of electrons resulting—for sufficiently large V_g values—in their depletion next to the surface. Under these conditions, electrons do not have enough kinetic energy to reach the surface, and suffer therefore less scattering processes. As a result their mobility increases. The same logic applies to holes for a sufficiently large positive $V_g > 0$ V [Fig. 2(d)]. We therefore expect that μ_e and μ_h should depend on V_g and exhibit opposite trends as the gate voltage is varied.

To confirm the validity of this physical scenario we perform a complete quantitative analysis of the measured gate-dependent classical magnetotransport in terms of an electron-hole two-band model. Changing V_g has a nonlocal and a local effect: it varies the mobility $\mu_{e,h}$ of electrons and holes in the bulk (nonlocal effect) without changing their density n and p, and it changes the density of charge carriers at the surface (within the electrostatic screening length, ≈1 nm, much smaller than the crystal thickness; local effect), which can also cause changes in the magnetotransport. In terms of the longitudinal and transverse square conductance $G_{\square,xx}$ and $G_{\square,xy}$ we then have

$$G_{\square,xx} = \sigma_{xx,\mathrm{bulk}}\, t + \sigma_{xx,\mathrm{inter}}, \tag{1}$$

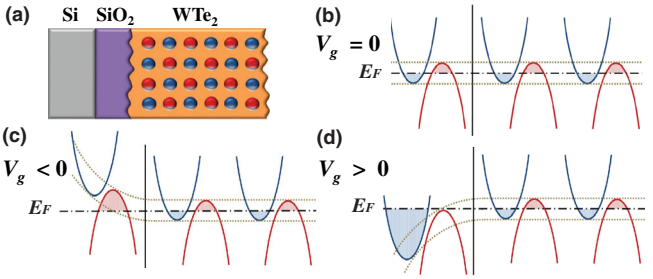

FIG. 2. (a) Schematic illustration of the device structure (the blue and red balls in the WTe_2 layer represent electrons and holes). (b)–(d) Band bending for different values of V_g. For $V_g = 0$ V (b) the system is uniform and electron and holes can reach the surface. For large negative V_g (c), electrons cannot reach the surface—where scattering processes predominantly occur—and their mobility increases. (d) The same holds true for holes at large positive V_g.

$$G_{\square,xy} = \sigma_{xy,\mathrm{bulk}} t + \sigma_{xy,\mathrm{inter}}, \quad (2)$$

where σ_{bulk} (σ_{inter}) is the 3D (2D) bulk (interface) conductivity. As discussed theoretically long ago [26,27], in the nonlocal transport regime occurring because of the presence of surface scattering, the carrier mobility $\mu_{e,h}$ and the (bulk) conductivity are defined as an average over crystal thickness t [e.g., $\mu_{e,h} = (1/t)\int_0^t \mu_{e,h}(z)dz$]. It is the introduction of these effective, averaged quantities that accounts for the nonlocality of the relation between current density and electric field, which is at the core of the phenomenon observed here (see Refs. [26–29]).

We discuss in detail the behavior of thick crystals in which the surface contribution, $\sigma_{xx,\mathrm{inter}}$ and $\sigma_{xy,\mathrm{inter}}$, can be entirely neglected with respect to the bulk one. This allows us to minimize the number of unknown parameters in the data analysis (the behavior of thinner crystals can also be reproduced in detail, as discussed in detail in the Supplemental Material [40]). By using the two-band model expressions for the bulk electron and hole classical conductivities Eqs. (1) and (2) reduce to [41,42]:

$$G_{\square,xx} = \sigma_{xx,\mathrm{bulk}} t = \left(\frac{pe\mu_h}{1+\mu_h^2 B^2} + \frac{ne\mu_e}{1+\mu_e^2 B^2}\right) t, \quad (3)$$

$$G_{\square,xy} = \sigma_{xy,\mathrm{bulk}} t = \left(\frac{pe\mu_h^2 B}{1+\mu_h^2 B^2} + \frac{ne\mu_e^2 B}{1+\mu_e^2 B^2}\right) t. \quad (4)$$

We first extract the (bulk) electron and hole density by fitting $G_{\square,xx}(B)$ and $G_{\square,xy}(B)$ at $V_g = 0$ V (see Ref. [22] for details). Then—as we change V_g—we keep n and p fixed to the value determined at $V_g = 0$ V and vary only μ_e and μ_h, to reproduce $G_{\square,xx}(B)$ and $G_{\square,xy}(B)$. As shown in Figs. 3(a)–3(b), the agreement between Eqs. (3) and (4) and the data is excellent throughout the V_g and B ranges investigated. In particular, Eq. (4) very successfully reproduces the nontrivial evolution of $G_{\square,xy}$ including its sign changes and the inversion of the slopes at low B. The values of $\mu_e(V_g)$ and $\mu_h(V_g)$ extracted from the fitting are plotted in Fig. 3(c), and exhibit the trends expected from the proposed physical scenario. The electron mobility increases as V_g becomes more negative, i.e., when electrons are pushed away from the interface, whereas the hole mobility exhibits the opposite behavior. The total change in either the electron or the hole mobility is less than a factor of 2, as it should be: even if scattering at one surface is fully suppressed, the nongated surface continues to limit the mobility. A similar quantitative analysis on six devices (out of more than 20 devices measured which exhibited the same trends) resulted in all cases in excellent agreement with Eqs. (1)–(4) and identical trends for the V_g dependence of $\mu_{e,h}$ (see Supplemental Material [40] for details). We therefore conclude that the observed unusual gate-induced variations of transport are caused by changes in the mobility of the bulk electrons and holes, and occur because of the nonlocal transport regime in which the devices operate [43].

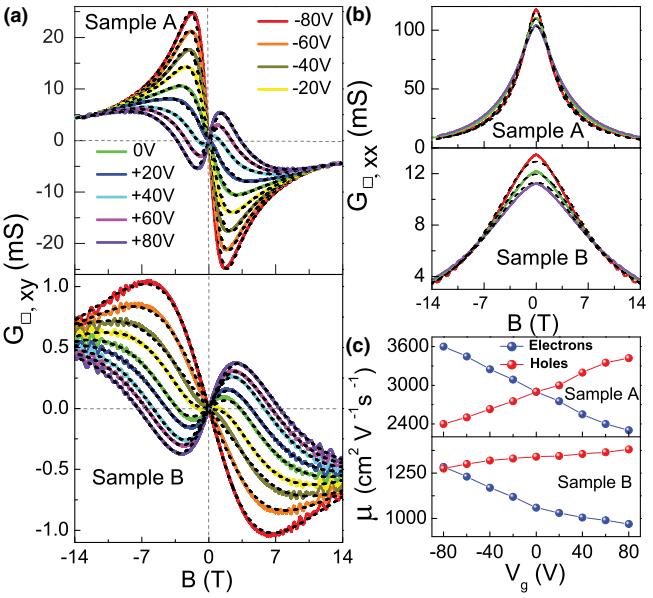

FIG. 3. Quantitative analysis of the gate-dependent magneto-transport through WTe_2 crystals of different thicknesses. (a), (b) Transverse and longitudinal square conductance, $G_{\square,xy}(B)$ and $G_{\square,xx}(B)$, of a 48 nm (sample A) and an 11 nm thick (sample B) crystal measured for different V_g at $T = 250$ mK. In all panels, curves of the same color correspond to the same value of V_g, as indicated by the legend in (a). The black dashed lines represent theoretical fits with Eqs. (1)–(4), which reproduce the data quantitatively in all detail. (c) V_g dependence of the electron (blue symbols) and hole (red symbols) mobility extracted from the analysis.

Such a field-effect mechanism had not been directly observed previously [38]. In semimetallic graphite or bismuth, for instance, a gate modulation of transport is routinely found in crystals with a thickness up to a few tens of nanometers [44–47]. In that case, however, the modulation of transport is due to the contribution to the conductivity given by the carriers accumulated near the surface, and for 50 nm or thicker crystals the effect is virtually negligible. In other kinds of transistors, a modulation of transport due to a gate-induced change in carrier mobility originating from the effect of surface roughness has been well documented [1,48]. In those transistors, however, carriers form a 2D conducting layer confined near the material surface, and the gate voltage does not influence the electronic properties in the interior of the material. The unique aspect of the field effect observed in our study of WTe_2 devices is that the gate voltage has an influence on the electronic properties over the entire material even for rather thick crystals.

To illustrate why the ability to gate tune the bulk properties of WTe_2 is particularly interesting, we discuss the effect of V_g on the (quantum) Shubnikov–de Haas

(SdH) oscillations originating from the formation of Landau levels in the bulk. The conventional theoretical expression describing the oscillatory component of ρ_{xx}, $\Delta\rho_{\rm osc}$ reads [49–53]

$$\frac{\Delta\rho_{\rm osc}}{\rho_{xx}} \propto \sqrt{\frac{\hbar eB}{m^* E_F}}\frac{X}{\sinh X}\exp\left(\frac{-\pi}{\mu B}\right)\sin\left(\frac{2\pi f}{B}\right), \tag{5}$$

where $X = (2\pi^2 k_B T m^*/\hbar eB)$, k_B is the Boltzmann constant, T is the temperature, and f is the oscillation frequency. From the analysis of classical transport, all parameters are known and we can use Eq. (5) to calculate the evolution of the SdH oscillations with V_g [54]. We then compare the Fourier spectrum obtained from the measured oscillations $\Delta\rho_{\rm osc}$ to that from the calculated $\Delta\rho_{\rm osc}^{\rm calc}$ by using Eq. (5) in the same B range of the measurements. Results for two different devices are shown in Figs. 4(a)–4(d): Figs. 4(a) and 4(c) illustrate the behavior of a device realized on an ~11 nm thick WTe_2 crystal with relatively low mobility, whereas Figs. 4(b) and 4(d) are from a high-mobility device ($\mu_{e,h} \sim 5.000$–6.000 cm^2 V^{-1} s^{-1}), whose behavior represents that of WTe_2 crystals that are 35–50 nm thick.

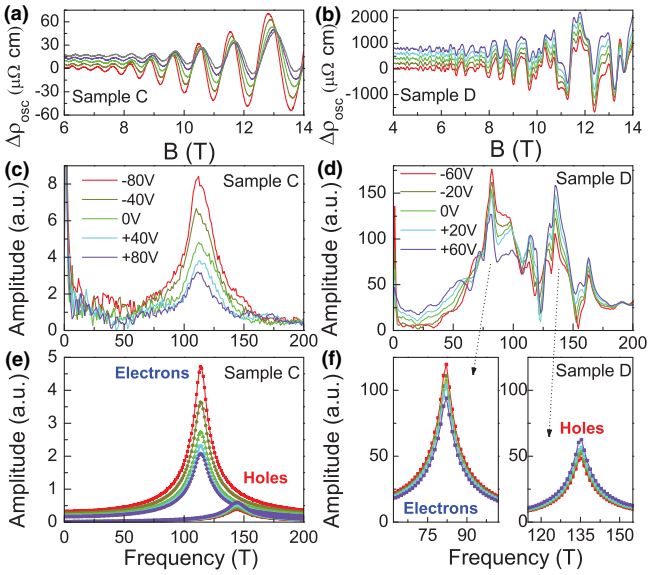

FIG. 4. Gate-dependent Shubnikov–de Haas (SdH) oscillations. (a), (b) Oscillatory component of the resistivity $\Delta\rho_{\rm osc}$—measured at $T = 250$ mK—for different values of V_g for two different devices, based on (a) a 11 nm (sample C) and (b) a 37 nm thick (sample D) WTe_2 crystals (the data have been offset for clarity). (c), (d) Fourier spectrum of the SdH oscillations shown in panels (a), (b). (e), (f) Fourier spectrum of the SdH oscillation $\Delta\rho_{\rm osc}^{\rm calc}$ calculated using Eq. (5) with the values of $\mu_e(V_g)$ and $\mu_h(V_g)$ extracted from the analysis of classical magnetotransport. Curves with the same color in panels (a), (c), (e) and (b), (d), (f) are taken at the same V_g indicated by the legends in panels (c) and (d), respectively.

The corresponding theoretical results are shown in Figs. 4(e)–4(f).

Starting with the thin device, Fig. 4(c) at $V_g = 0$ V shows a single broad peak at $f \sim 114$ T, with a faint shoulder at $f \sim 144$ T (see also the data from sample E shown in the Supplemental Material [40]). Upon changing V_g, the positions of the peak and shoulder do not change, since the bulk density is unaffected by V_g. The amplitude of the peak, on the contrary, changes considerably, consistently with the change in carrier mobility. Since at more positive V_g μ_e decreases and μ_h increases, the strong suppression with increasing V_g indicates that the peak originates from SdH oscillations of electrons. For comparison, Fig. 4(e) shows the spectrum obtained from Eq. (5) using the values of $\mu_e(V_g)$ and $\mu_h(V_g)$ extracted from the analysis of classical transport on the same device. The trend of the theoretically calculated and experimentally measured curves matches satisfactorily: electron SdH oscillations have a stronger V_g dependence, while hole SdH oscillations (responsible for the shoulder at $f \sim 144$ T; see Supplemental Material [40]) exhibit a much smaller V_g dependence due to their lower mobility and larger effective mass. Most typically, especially in the thin devices, $\mu_e > \mu_h$ and SdH oscillations exhibit predominantly the V_g dependence expected for electrons.

In the highest mobility devices, however, both electron and hole SdH oscillations are clearly visible in the experiments [Fig. 4(d)]. The evolution of the spectrum with increasing V_g from −60 to 60 V is opposite in different frequency ranges. For 75 T $< f <$ 105 T, the spectrum amplitude decreases upon increasing V_g, consistently with SdH oscillations caused by electrons, whereas for 115 T $< f <$ 165 T the opposite trend is clearly visible, as expected for holes. The fine structure present in the spectrum (usually seen in devices having this mobility and thickness, and possibly originating from size quantization generating multiple electron and hole subbands) prevents a quantitative comparison. Nevertheless, with $\mu_e(V_g)$ and $\mu_h(V_g)$ extracted from the classical magnetotransport analysis, Eq. (5) predicts that the relative variations in the electron and hole contributions induced by V_g are comparable in magnitude [Fig. 4(f)], as found in the experiments. We conclude that—for sufficiently high-mobility devices—the gate dependence allows the identification of the carriers responsible for the SdH oscillations observed at a certain frequency.

In conclusion, we have observed and explained a long-range field effect of magnetotransport in WTe_2 originating from the gate-voltage dependence of the mobility of bulk electrons and holes, caused by surface scattering. Our observations demonstrate the possibility to gate control the electronic properties of a material well inside its interior, over a depth much larger than the electrostatic screening length. This finding can be relevant for the

hydrodynamics of ballistic electrons [55]—since the gate tuning effect of surface scattering may give control over the viscosity of the electron-hole liquid—which has attracted enormous interest in recent times [56–58].

We acknowledge A. Ferreira for technical help. Financial support from the Swiss National Sicence Foundation, the NCCR QSIT, and the EU Graphene Flagship project is also acknowledged.

[1] C. H. Ahn *et al.*, Rev. Mod. Phys. **78**, 1185 (2006).
[2] H. Ohno, D. Chiba, F. Matsukura, T. Omiya, E. Abe, T. Dietl, Y. Ohno, and K. Ohtani, Nature (London) **408**, 944 (2000).
[3] K. S. Novoselov *et al.*, Science **306**, 666 (2004).
[4] R. Martel, T. Schmidt, H. R. Shea, T. Hertel, and P. Avouris, Appl. Phys. Lett. **73**, 2447 (1998).
[5] A. D. Caviglia, S. Gariglio, N. Reyren, D. Jaccard, T. Schneider, M. Gabay, S. Thiel, G. Hammerl, J. Mannhart, and J.-M. Triscone, Nature (London) **456**, 624 (2008).
[6] M. N. Ali *et al.*, Nature (London) **514**, 205 (2014).
[7] I. Pletikosić, M. N. Ali, A. V. Fedorov, R. J. Cava, and T. Valla, Phys. Rev. Lett. **113**, 216601 (2014).
[8] J. Jiang *et al.*, Phys. Rev. Lett. **115**, 166601 (2015).
[9] Z. Zhu, X. Lin, J. Liu, B. Fauqué, Q. Tao, C. Yang, Y. Shi, and K. Behnia, Phys. Rev. Lett. **114**, 176601 (2015).
[10] D. Rhodes, S. Das, Q. R. Zhang, B. Zeng, N. R. Pradhan, N. Kikugawa, E. Manousakis, and L. Balicas, Phys. Rev. B **92**, 125152 (2015).
[11] Y. Zhao *et al.*, Phys. Rev. B **92**, 041104 (2015).
[12] P. L. Cai, J. Hu, L. P. He, J. Pan, X. C. Hong, Z. Zhang, J. Zhang, J. Wei, Z. Q. Mao, and S. Y. Li, Phys. Rev. Lett. **115**, 057202 (2015).
[13] X.-C. Pan *et al.*, Nat. Commun. **6**, 7805 (2015).
[14] D. Kang *et al.*, Nat. Commun. **6**, 7804 (2015).
[15] L. R. Thoutam, Y. L. Wang, Z. L. Xiao, S. Das, A. Luican-Mayer, R. Divan, G. W. Crabtree, and W. K. Kwok, Phys. Rev. Lett. **115**, 046602 (2015).
[16] Y. Wu, N. H. Jo, M. Ochi, L. Huang, D. Mou, S. L. Bud'ko, P. C. Canfield, N. Trivedi, R. Arita, and A. Kaminski, Phys. Rev. Lett. **115**, 166602 (2015).
[17] Y. L. Wang *et al.*, Phys. Rev. B **92**, 180402 (2015).
[18] Y. M. Dai *et al.*, Phys. Rev. B **92**, 161104 (2015).
[19] C. C. Homes, M. N. Ali, and R. J. Cava, Phys. Rev. B **92**, 161109 (2015).
[20] W.-D. Kong, S.-F. Wu, P. Richard, C.-S. Lian, J.-T. Wang, C.-L. Yang, Y.-G. Shi, and H. Ding, Appl. Phys. Lett. **106**, 081906 (2015).
[21] P. K. Das *et al.*, Nat. Commun. **7**, 10847 (2016).
[22] L. Wang, I. Gutiérrez-Lezama, C. Barreteau, N. Ubrig, E. Giannini, and A. F. Morpurgo, Nat. Commun. **6**, 8892 (2015).
[23] P. S. Alekseev, A. P. Dmitriev, I. V. Gornyi, V. Y. Kachorovskii, B. N. Narozhny, M. Schütt, and M. Titov, Phys. Rev. Lett. **114**, 156601 (2015).
[24] A. A. Soluyanov, D. Gresch, Z. Wang, Q. Wu, M. Troyer, X. Dai, and B. A. Bernevig, Nature (London) **527**, 495 (2015).
[25] X. Qian, J. Liu, L. Fu, and J. Li, Science **346**, 1344 (2014).
[26] E. H. Sondheimer, Adv. Phys. **1**, 1 (1952).
[27] J. R. Schrieffer, Phys. Rev. **97**, 641 (1955).
[28] P. J. Price, IBM J. Res. Dev. **4**, 152 (1960).
[29] H. Ibach, *Physics of Surfaces and Interfaces* (Springer, Berlin, 2006), pp. xii, 646.
[30] H. Fu, K. V. Reich, and B. I. Shklovskii, Phys. Rev. B **94**, 045310 (2016).
[31] H. Fu, K. V. Reich, and B. I. Shklovskii, Phys. Rev. B **93**, 235312 (2016).
[32] The nonlocality that we are referring to is described by a relation between current density $\vec{J}$ and electrical field $\vec{E}$, of the type $\vec{J}(x) = \int dy \sigma(x,y)\vec{E}(y)$.
[33] G. E. H. Reuter and E. H. Sondheimer, Proc. R. Soc. A **195**, 336 (1948).
[34] R. G. Chambers, Nature (London) **165**, 239 (1950).
[35] R. G. Chambers, Proc. R. Soc. A **215**, 481 (1952).
[36] A. Berman and H. Juretschke, Appl. Phys. Lett. **18**, 417 (1971).
[37] A. Berman and H. J. Juretschke, Phys. Rev. B **11**, 2903 (1975).
[38] In Refs. [36,37] the observation of a (gate-induced) 10^{-5} relative change in the conductivity of metallic thin films was claimed to represent a manifestation of these phenomena. However, no actual evidence for a long-range field effect was presented, as the claim was entirely based on data interpretation (using the phenomenological Fuchs-Sondheimer model) and not on direct measurements. It is now known that the assumptions made in Refs. [36,37] are wrong and so are the conclusions [thorough discussions of this issue can be found in numerous papers, including A. F. Mayadas *et al.*, Appl. Phys. Lett. **14**, 345 (1969); A. F. Mayadas and M. Shatzkes, Phys. Rev. B **1**, 1382 (1970); R. C. Munoz *et al.*, Phys. Rev. B **62**, 4686 (2000)].
[39] For sample A, for instance, $\mu_e = 2.900\ \mathrm{cm^2\,V^{-1}\,s^{-1}}$ and $\mu_h = 2.900\ \mathrm{cm^2\,V^{-1}\,s^{-1}}$, so that the electron and hole mean free paths $L_h \sim L_e \sim 0.3\ \mu\mathrm{m} \gg t$; the Fermi vector k_F is estimated from Refs. [7–10].
[40] See Supplemental Material at http://link.aps.org/supplemental/10.1103/PhysRevLett.117.176601 for the details of the quantitative analysis of classical magnetotransport behavior and the gate-dependent Shubnikov–de Hass oscillations in WTe_2.
[41] S. S. Murzin, S. I. Dorozhkin, G. Landwehr, and A. C. Gossard, JETP Lett. **67**, 113 (1998).
[42] E. H. Sondheimer and A. H. Wilson, Proc. R. Soc. A **190**, 435 (1947).
[43] This conclusion is confirmed by the observation, discussed in the Supplemental Material [40], that when the exposure to ambient of the WTe_2 crystals is only very limited—so that only minor surface degradation occurs—no gate-voltage dependence of transport is observed experimentally. In general, the magnitude of the field effect that we observe depends on the amount of surface degradation which is determined by details of the fabrication process.
[44] Y. Zhang, J. P. Small, M. E. S. Amori, and P. Kim, Phys. Rev. Lett. **94**, 176803 (2005).
[45] Y. Zhang, J. P. Small, W. V. Pontius, and P. Kim, Appl. Phys. Lett. **86**, 073104 (2005).
[46] A. V. Butenko, V. Sandomirsky, Y. Schlesinger, D. Shvarts, and V. A. Sokol, J. Appl. Phys. **82**, 1266 (1997).
[47] A. V. Butenko, D. Shvarts, V. Sandomirsky, and Y. Schlesinger, Appl. Phys. Lett. **75**, 1628 (1999).

[48] T. Ando, A. B. Fowler, and F. Stern, Rev. Mod. Phys. **54**, 437 (1982).
[49] F. E. Richards, Phys. Rev. B **8**, 2552 (1973).
[50] H. H. J. M. Niederer, Jpn. J. Appl. Phys. **13**, 339 (1974).
[51] I. Eisele, H. Gesch, and G. Dorda, Surf. Sci. **58**, 169 (1976).
[52] F. F. Fang, A. B. Fowler, and A. Hartstein, Phys. Rev. B **16**, 4446 (1977).
[53] A. F. Bangura *et al.*, Phys. Rev. Lett. **100**, 047004 (2008).
[54] For the electron-hole effective masses we use $m_e^* = 0.5m_0$, $m_h^* = 1.0m_0$, in the range of values reported in the literature [7–10]; $m_e^* = 0.33 \sim 0.51m_0$ and $m_h^* = 0.42 \sim 1.1m_0$, with m_0 the free electron mass; for f, we insert the observed value.
[55] M. J. M. de Jong and L. W. Molenkamp, Phys. Rev. B **51**, 13389 (1995).
[56] D. A. Bandurin *et al.*, Science **351**, 1055 (2016).
[57] J. Crossno *et al.*, Science **351**, 1058 (2016).
[58] P. J. W. Moll, P. Kushwaha, N. Nandi, B. Schmidt, and A. P. Mackenzie, Science **351**, 1061 (2016).